NAVAL POSTGRADUATE SCHOOL

Monterey, California

THESIS

EFFECTS OF VIDEO BANDWIDTH ON
THE PERFORMANCE OF A SQUARE LAW DETECTOR
WITH GAUSSIAN IF AND VIDEO FILTERS

by

Chang Long Wee

September, 1991

Thesis Advisor: D.v.Z. Wadsworth

Approved for public release; distribution is unlimited

REPORT DOCUMENTATION PAGE

1a. REPORT SECURITY CLASSIFICATION UNCLASSIFIED	1b. RESTRICTIVE MARKINGS
2a. SECURITY CLASSIFICATION AUTHORITY	3. DISTRIBUTION/AVAILABILITY OF REPORT Approved for public release; distribution is unlimited.
2b. DECLASSIFICATION/DOWNGRADING SCHEDULE	
4. PERFORMING ORGANIZATION REPORT NUMBER(S)	5. MONITORING ORGANIZATION REPORT NUMBER(S)
6a. NAME OF PERFORMING ORGANIZATION Naval Postgraduate School 6b. OFFICE SYMBOL (*If applicable*) EC	7a. NAME OF MONITORING ORGANIZATION Naval Postgraduate School
6c. ADDRESS (*City, State, and ZIP Code*) Monterey, CA 93943-5000	7b. ADDRESS (*City, State, and ZIP Code*) Monterey, CA 93943-5000
8a. NAME OF FUNDING/SPONSORING ORGANIZATION 8b. OFFICE SYMBOL (*If applicable*)	9. PROCUREMENT INSTRUMENT IDENTIFICATION NUMBER
8c. ADDRESS (*City, State, and ZIP Code*)	10. SOURCE OF FUNDING NUMBERS Program Element No / Project No / Task No / Work Unit Accession Number

11. TITLE (*Include Security Classification*)
EFFECTS OF VIDEO BANDWIDTH ON THE PERFORMANCE OF A SQUARE LAW DETECTOR WITH GAUSSIAN IF AND VIDEO FILTERS

12. PERSONAL AUTHOR(S) Chang Long Wee

13a. TYPE OF REPORT	13b. TIME COVERED	14. DATE OF REPORT (*year, month, day*)	15. PAGE COUNT
Master's Thesis	From To	1991, September	69

16. SUPPLEMENTARY NOTATION
The views expressed in this thesis are those of the author and do not reflect the official policy or position of the Department of Defense or the U.S. Government.

17. COSATI CODES			18. SUBJECT TERMS (*continue on reverse if necessary and identify by block number*)
FIELD	GROUP	SUBGROUP	Square law detector; Gaussian filter; cumulants; probability density functions; Emerson's method; receiver operating characteristics; collapsing ratio; collapsing loss.

19. ABSTRACT (*continue on reverse if necessary and identify by block number*)

The effects of Gaussian-shaped IF and video filters on the performance of a square-law detector employing post-detection integration are analyzed. The number of additional noise-only samples that are integrated due to a finite video bandwidth is determined. Emerson's method is used to obtain an expression for the cumulants of the output probability density function. These cumulants are used in Edgeworth's asymptotic series expansion of the density functions. By integrating these density functions, the receiver operating characteristics are determined for various values of IF bandwidth to video bandwidth. A collapsing ratio which takes into account the Gaussian shape of the filters is formulated and compared against Barton's approximate formula for the collapsing ratio. For typical video bandwidths, Barton's approximate formula is found to overestimate the collapsing loss by amount less than 0.5 dB.

20. DISTRIBUTION/AVAILABILITY OF ABSTRACT ☒ UNCLASSIFIED/UNLIMITED ☐ SAME AS REPORT ☐ DTIC USERS	21. ABSTRACT SECURITY CLASSIFICATION Unclassified	
22a. NAME OF RESPONSIBLE INDIVIDUAL Donald v.Z. Wadsworth	22b. TELEPHONE (*Include Area code*) (408) 646-2115	22c. OFFICE SYMBOL EC/Wd

DD FORM 1473, 84 MAR 83 APR edition may be used until exhausted
All other editions are obsolete

Approved for public release; distribution is unlimited.

Effects of Video Bandwidth on the Performance of a Square Law Detector with Gaussian IF and Video Filters

by

Chang Long Wee
Major, Republic of Singapore Air Force
B.E.E., National University of Singapore, 1983

Submitted in partial fulfillment
of the requirements for the degree of

MASTER OF SCIENCE IN ELECTRICAL ENGINEERING

from the

NAVAL POSTGRADUATE SCHOOL
September 1991

ABSTRACT

The effects of Gaussian-shaped IF and video filters on the performance of a square-law detector employing post-detection integration are analyzed. The number of additional noise-only samples that are integrated due to a finite video bandwidth is determined. Emerson's method is used to obtain an expression for the cumulants of the output probability density function. These cumulants are used in Edgeworth's asymptotic series expansion of the density functions. By integrating these density functions, the receiver operating characteristics are determined for various ratios of IF bandwidth to video bandwidth. A collapsing ratio which takes into account the Gaussian shape of the filters is formulated and compared against Barton's approximate formula for the collapsing ratio. For typical video bandwidths, Barton's approximate formula is found to overestimate the collapsing loss by an amount less than 0.5 dB.

TABLE OF CONTENTS

I. INTRODUCTION

This report is concerned with the effects of insufficient video bandwidth on the detection performance of a square law detector with Gaussian-shaped intermediate frequency (IF) and video filters in pulsed radar applications.

The square-law detector is assumed to have an arbitrary wide low-pass zonal filter [Ref. 1] so that its instantaneous output is just the square of the envelope of the input signal. This assumption is in line with Marcum's definition of the detector as "any device whose instantaneous output is a function of the envelope of the input wave only" [Ref. 2].

In most practical radars with superheterodyne receivers, the second detector is usually followed by one or more stages of video amplification prior to post-detection integration and threshold detection. The bandwidth of the video amplifier must be sufficiently wide to avoid distortion of the input video signal from the detector. It has been pointed out that the video bandwidth B_v must be greater than one-half the IF bandwidth B_{if} to be "sufficiently wide" [Ref. 3]. In practice, the video bandwidth may be less than half the IF bandwidth.

An insufficient video bandwidth will have two effects on the detection statistics of the radar receiver. Firstly, it

will affect the threshold setting for a specified probability of false alarm, P_{fa}. Secondly, it will adversely affect the input signal-to-noise ratio required to attain a desired probability of detection, P_d, for a specified probability of false alarm. An equivalent statement to the second effect is that there will be a degradation in probability of detection vis-a-vis the probability of detection attainable with an ideal video bandwidth for the same signal-to-noise ratio and probability of false alarm.

The focus of this report will be on the degradation in performance associated with the second effect. Mathematically, Marcum [Ref. 2] has treated this degradation in performance by modelling it as a consequence of integrating M additional noise-only samples along with the desired N signal-plus-noise samples[1]. The degradation in performance is quantified by introducing a "collapsing loss", L_c, which has been defined in dB as the incremental increase in signal-to-noise ratio with respect to the signal-to-noise ratio required in the ideal case of integrating only signal-plus-noise samples for the

---

[1]Marcum's paper first introduced the general concept of a collapsing loss resulting from the integration of a greater number of noise-only samples than signal-plus-noise samples. Insufficient video bandwidth is treated, among others, as a specific cause of collapsing loss.

same probability of detection. Mathematically, this is expressed as: [Ref. 4]

$$L_c \; dB = X_{N+M} \; dB - X_N \; dB \qquad (1)$$

where X_{N+M} is the signal-to-noise ratio required when N signal-plus-noise samples plus M extra noise samples are integrated, and X_N is the signal-to-noise ratio required when only N signal-plus-noise samples are integrated.

The signal-plus-noise samples and noise-only samples are assumed to be independent and respectively identically distributed.

Mathematically, Marcum showed that for a non-fluctuating target, the effect on the detection statistics of integrating M additional noise samples can be taken into account by multiplying the joint characteristic function of the N signal-plus-noise samples by the joint characteristic function of the M noise-only samples. Defining the collapsing ratio,

$$\rho = \frac{M + N}{N} \qquad (2)$$

Marcum showed that for the square law detector

$$C_{N+M}(\xi) = \frac{\exp\left[-N\rho \left(\frac{X}{\rho}\right) \left(\frac{j\xi}{1+j\xi}\right) \right]}{(1+j\xi)^{N\rho}} \qquad (3)$$

where $C_{N+M}(\xi)$ is the characteristic function for the joint density function of N signal-plus-noise samples plus M additional noise samples.

When ρ is equal to one (i.e., M is equal to zero), Eqn (3) reduces to the equation of the characteristic function with no collapsing loss, i.e.,

$$C_N(\xi) = \frac{\exp\left[-NX\left(\frac{j\xi}{1+j\xi}\right) \right]}{(1+j\xi)^N} \qquad (4)$$

Comparing Eqn (3) with Eqn (4), it is seen that the statistical results for $\rho = 1$ can be easily extended for any ρ. In particular, receiver operating characteristics (ROC) such as Meyer plots[2] for $\rho = 1$ are available in the literature and can be used directly to determine the signal-to-noise required by using ρN instead of N as the number of pulses integrated and with $\frac{X}{\rho}$ as a parameter of the ROC instead of X. [Ref. 4]

---

[2]These are plots of P_D as a function of the number of pulses noncoherently integrated for a given Fehlner's false alarm number and with the input signal-to-noise ratio for a single pulse as a running parameter.

Hence, the quantitative effects on the detection statistics of insufficient video bandwidth can be determined once the collapsing ratio, ρ, is known. The problem is in relating M (and hence, ρ) to the video bandwidth. What is the effective number of additional noise-only samples that are integrated along with the intended number of signal-plus-noise samples given a finite video bandwidth?

A common practice is to use the following semi-empirical formula given by Barton [Ref. 5] to estimate the collapsing ratio:

$$\rho_B = \frac{B_{if} + 2B_v}{2B_v} \tag{5}$$

where the IF noise equivalent bandwidth B_{if} is assumed to be matched to the pulse width such that $B_{if}\tau = 1$. The video filter is modeled as an ideal low-pass filter with a flat frequency response from $-B_v$ to $+B_v$ and zero elsewhere. The frequency response characteristics of the actual filter is not taken into account apart from computing its noise-equivalent bandwidth, B_v.

The purpose of this paper is to investigate the effects of Gaussian-shaped IF and video filters on the detection performance of the square-law detector. The primary consideration in the choice of Gaussian-shaped filters for this investigation is the mathematical convenience of the

Gaussian shape which yields analytical results in closed form.

Although a Gaussian filter is physically not realizable, it has been found to be a good approximation in characterizing the frequency response of multistage RC amplifiers [Ref. 6]. Hence, the results obtained will have direct application for square-law detectors with multistage pre-detection and post-detection RC filters, besides providing a relative measure of the accuracy of Barton's formula for the collapsing ratio.

In the next section, the effects of video bandwidth on the detector's output probability density functions and operating characteristics will be analyzed. Specifically, a formula will be developed to determine the additional noise-only samples integrated due to a finite video bandwidth. This leads to the formulation of the collapsing ratio which will be discussed and compared against Barton's formula in Section III. Section IV summarizes the methods and findings of this paper.

II. DEGRADATION IN PERFORMANCE

A. DESCRIPTION OF THE SYSTEM

The system under consideration is illustrated in Figure 1. It consists of a Gaussian IF filter, a square-law detector, a video amplifier with a Gaussian frequency response, and a linear post-detection integrator. For convenience, it shall be referred to as the Gaussian square-law system.

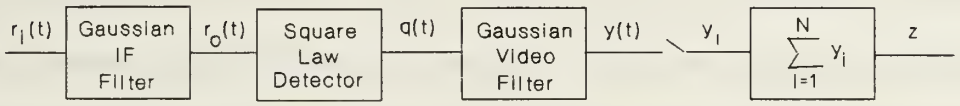

Figure 1. Block diagram of the Gaussian square-law system.

The IF filter has a Gaussian passband characteristic with a center frequency of f_o and a root-mean-square bandwidth of β. The video amplifier also has a Gaussian passband but with a root-mean-square bandwidth of ν centered at zero frequency. Since the gain of the video amplifier will have no impact on detection performance, it is assumed to have unity gain for mathematical convenience. Correspondingly, the impulse response functions of the IF filter and video amplifier are

respectively defined by:

$$h_{if}(t) = 2(2\pi\beta^2)^{\frac{1}{2}} \exp[-(2\pi\beta)^2 \frac{t^2}{2}] \cos\omega_o t \qquad (6)$$

and

$$h_v(t) = (2\pi\nu^2)^{\frac{1}{2}} \exp[-(2\pi\nu)^2 \frac{t^2}{2}] \qquad (7)$$

The signal to be detected is a pulse-modulated sinusoidal waveform corresponding to the echo from a target at a particular range from the radar.

The input noise to the system is assumed to be additive white Gaussian noise (AWGN) with a two-sided power spectral density equal to $\eta/2$. The noise-equivalent bandwidth of the IF filter, B_{if}, is matched to the pulse width so that noise at the input to the detector can be assumed to be completely uncorrelated from pulse to pulse [Ref. 2].

B. ADDITIONAL NOISE-ONLY SAMPLES INTEGRATED

For the hypothetical case of infinite video bandwidth, the video range bins will have the same resolution as the IF range bins, which is of the order of one pulse width. However, for most practical video amplifiers with finite bandwidths, the resolution of the video range bins will be poorer than those of the IF range bins. In such cases, each sampled output of the video amplifier will be shown in the subsequent paragraphs

to be equivalent to the result of averaging N_v independent samples of the detector output, where N_v is a number greater than one. Since the detector follows a square law, each of the N_v independent samples is equal to the square of the voltage envelope in the corresponding IF range bins.

Suppose a target is present at a particular IF range bin. One of the N_v samples will consist of signal-plus-noise. The remaining N_v-1 samples will consist of noise only. Hence, N_v-1 additional noise-only samples will be integrated for every signal-plus-noise sample integrated. The added noise results in a degradation in performance that is quantified by a collapsing loss.

The number of noise-only samples integrated along with the signal-plus-noise sample can be determined by recognizing that the video amplifier with a finite bandwidth behaves as an analog filter integrator and paralleling it with a digital integrator that averages N_v independent samples of the detector output. This is illustrated in Figure 2.

The digital integrator as shown in Figure 2(a) has the well-known effect of decreasing the variance of the input samples, q_j, by a factor of N_v, i.e.,

$$Var\{y\} = \frac{Var\{q_j\}}{N_v} \qquad (8)$$

where y is the output of the digital integrator.

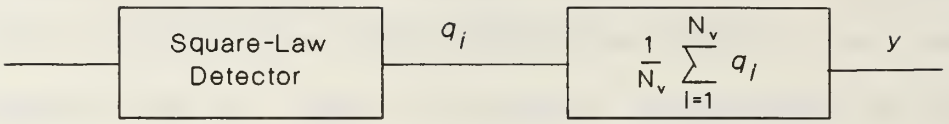

(a) Digital Integrator: $Var(y) = Var(q)/N_v$

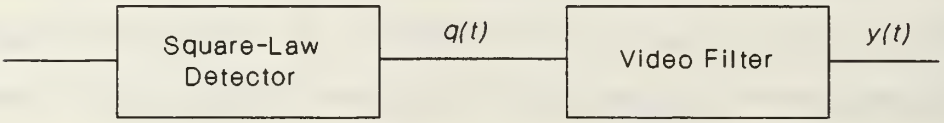

(b) Video filter: Equivalent $N_v = Var\{q(t)\}/Var\{y(t)\}$

Figure 2. Equivalent number of independent samples averaged by the video filter.

Hence, the equivalent number of samples, N_v, averaged by the video filter can be determined by evaluating:

$$N_v = \frac{Var\{q(t)\}}{Var\{y(t)\}} \qquad (9)$$

where

$q(t)$ = output of the square-law detector

$y(t)$ = output of the video filter (amplifier).

The cumulants of the probability density function (pdf) f_y at the output of the Gaussian video filter can be determined by the method of Emerson [Ref. 7]. When the input to the square law detector is a CW sinusoidal signal contaminated by

AWGN, the cumulants are given by:

$$K_{y,r} = \frac{(2\sigma^2)^r\,(r-1)!}{[(1+2\gamma^2)^{\frac{1}{2}}+1]^r - [(1+2\gamma^2)^{\frac{1}{2}}-1]^r} \times \tag{10}$$

$$\left[1 + rX' \sqrt{\frac{[(1+2\gamma^2)^{\frac{1}{2}}+1]^r - [(1+2\gamma^2)^{\frac{1}{2}}-1]^r}{[(1+2\gamma^2)^{\frac{1}{2}}+1]^r + [(1+2\gamma^2)^{\frac{1}{2}}-1]^r}}\,(1+2\gamma^2)^{\frac{1}{4}}\right]$$

where

$K_{y,r}$ = rth cumulant of the pdf, f_y

σ^2 = average noise power at the input to the detector

X' = signal-to-noise ratio at the input to the detector

$\gamma = \frac{B_{if}}{2B_v}$

The mathematical derivation of Eqn (10) is shown in Appendix A. For the purpose of this Section, it is sufficient to point out that the derivation takes into account the shape of the Gaussian filter and that the cumulants are in general related to the characteristic function of the associated probability density function by the following definition [Ref. 8]:

$$\exp\left[\sum_{r=1}^{\infty} \frac{K_r (j\xi)^r}{r!}\right] = C(\xi) \tag{11}$$

The cumulants are also related to the central moments of the density function.[3] In particular, the variance or second central moment of the density function is equal to the second cumulant of the density function.

Hence, for the case of a CW sinusoidal signal,

$$Var\{y(t)\} = K_{y,2} = \frac{\sigma^2}{\sqrt{1+2\gamma^2}} \left[1 + 2X' \sqrt{\frac{1+2\gamma^2}{1+\gamma^2}} \right] \qquad (12)$$

To use Eqn (12) for evaluating N_v in Eqn (9), X' must be the equivalent CW signal-to-noise ratio that will produce the same variance resulting from the averaging of one signal-plus-noise sample and N_v-1 noise-only samples.

Referring to Figure 2(a), let X be the input signal-to-noise ratio of the jth range bin containing the target. Then,

$$y = \frac{1}{N_v} q_j + \frac{1}{N_v} \sum_{\substack{i=1 \\ i \neq j}}^{N_v} q_i \qquad (13)$$

and

$$Var\{y\} = \frac{1}{N_v^2} Var\{q_j\} + \frac{N_v - 1}{N_v^2} Var\{q_i\}, \quad i \neq j \qquad (14)$$

---

[3]A full treatment of the relationship between the cumulants and the moments of the probability density function can be found in Ref. 8.

where q_i are independent and identically distributed noise-only samples for $i = j$.

Now, q_i is the output of the square-law detector prior to any video filtering. For analysis, this is theoretically equal to the output y when the video filter has an infinite bandwidth. Hence,

$$Var\{q_j\} = K_{y,2}\Big|_{\gamma=0, X'=X} \qquad (15)$$

$$= \sigma^2(1+2X)$$

and

$$Var\{q_i\} = K_{y,2}\Big|_{\gamma=0, X'=0} \qquad (16)$$

$$= \sigma^2$$

Substituting the above results into Eqn (14) and simplifying yields the following expression for the variance of y:

$$Var\{y\} = \frac{2\sigma^2}{N_v^2}X + \frac{\sigma^2}{N_v} \qquad (17)$$

Let $\overline{X}$ be the equivalent signal-noise-ratio in each of the N_v range bins that will produce the same variance resulting from averaging the single signal-plus-noise sample with N_v noise-only samples.

Then, using Eqn (12) with $\gamma = 0$ and $X' = \bar{X}$, it follows that

$$Var\{q_j\} = \sigma^2 (1 + 2\bar{X}) \tag{18}$$

and

$$Var\{Y\} = Var\left[\frac{1}{N_v} \sum_{i=1}^{N_v} q_i\right] \tag{19}$$

$$= \frac{\sigma^2}{N_v} (1 + 2\bar{X})$$

By equating Eqn (17) and Eqn (19), it can be easily shown that

$$\bar{X} = \frac{X}{N_v} \tag{20}$$

Hence, for an arbitrary γ, it follows from Eqn (12) and Eqn (20) that

$$Var\{y(t)\} = K_{y,2}\Big|_{X'=\bar{X}} \tag{21}$$

$$= \frac{\sigma^2}{\sqrt{1+2\gamma^2}} \left[1 + 2\frac{X}{N_v}\sqrt{\frac{1+2\gamma^2}{1+\gamma^2}}\right]$$

The equivalent number of independent samples N_v averaged by the video filter can now be determined by using Eqn (9), i.e.,

$$N_v = \frac{Var\{q(t)\}}{Var\{y(t)\}} \tag{22}$$

with

$$Var\{y(t)\} = \frac{\sigma^2}{\sqrt{1+2\gamma^2}}\left[1 + 2\frac{X}{N_v}\sqrt{\frac{1+2\gamma^2}{1+\gamma^2}}\right] \tag{23}$$

and

$$Var\{q(t)\} = \sigma^2\left(1+\frac{2X}{N_v}\right) \tag{24}$$

Substituting Eqn (23) and Eqn (24) into Eqn (22) results in the following quadratic expression in N_v:

$$N_v^2 + \left[2X\sqrt{\frac{1+2\gamma^2}{1+\gamma^2}} - \sqrt{1+2\gamma^2}\right]N_v - 2X\sqrt{1+2\gamma^2} = 0 \tag{25}$$

Hence, the equivalent number of independent samples averaged by the Gaussian-shaped video filter is given by:

$$N_v = \frac{-b + \sqrt{b^2-4c}}{2} \tag{26}$$

where

$$b = 2X\sqrt{\frac{1+2\gamma^2}{1+\gamma^2}} - \sqrt{1+\gamma^2} \tag{27}$$

and

$$c = -2X\sqrt{1+2\gamma^2} \tag{28}$$

Solving Eqn (26) for $\gamma = 0$ shows that N_v is equal to one when the video bandwidth is infinitely large. This result is consistent with the earlier observation that the video range bins will have the same resolution as the IF range bins when the video bandwidth is infinite.

C. RECEIVER OPERATING CHARACTERISTICS

The collapsing loss caused by insufficient video bandwidth can be observed by examining the effect of integrating the additional noise-only samples on the output probability density function and operating characteristics of the Gaussian square law system.

The number of signal-plus-noise samples N integrated by the post-detection integrator corresponds to the number of pulses returned from a target as the radar antenna scans through its beamwidth [Ref. 3]. For most practical radars, this number is sufficiently large so that the probability density function of the voltage at the output of the linear post-detection integrator shown in Figure 1 tends towards a

normal distribution which can be asymptotically expanded using Edgeworth's groupings of the Gram-Charlier series expansion [Ref. 9, Ref. 10]:

$$f_Z(z) \simeq \Big[\phi(z') - \frac{C_1}{6}\phi^{(3)}(z') + \frac{C_2}{24}\phi^{(4)}(z') + \frac{C_1^2}{72}\phi^{(6)}(z') - \frac{C_3}{120}\phi^{(5)}(z') - \frac{C_1 C_2}{144}\phi^{(7)}(z') - \frac{C_1^3}{1296}\phi^{(9)}(z') + \ldots\ldots \Big] \times \frac{\sigma}{\sqrt{NK_{y,2}}} \tag{29}$$

where the terms on each line within the brackets are of the same order of magnitude [Ref. 11]; and

z = integrator output voltage normalized by the rms noise voltage σ at the input to the detector.

$$z' = \frac{\sigma z - NK_{y,1}}{\sqrt{NK_{y,2}}} \tag{30}$$

$$\Phi(z) = \frac{1}{\sqrt{2\pi}} \exp\left[-\frac{z^2}{2}\right] \tag{31}$$

$$\phi^{(m)}(z) = (-1)^m \phi(z) H_m(z) \qquad (32)$$

$H_m(z)$ = mth order Hermite polynomial in z

$$C_r = \frac{1}{N^{0.5r}} \frac{K_{y,r+2}}{(K_{y,2})^{1+0.5r}} \qquad (32)$$

The symbol $K_{y,r}$ denotes the rth cumulant of the probability density function of the video filter output y which takes into account the additional noise-only samples averaged along with each signal-plus-noise sample.

Studies by Cramer [Ref. 11] have validated the asymptotic behaviour of Edgeworth's series and determined that in general, the remainder term of the expansion is of the same order as the first term neglected. Hence, the output probability density function $f_z(z)$ can be expanded to the desired order of accuracy once the cumulants $K_{y,r}$ are known.

The cumulants $K_{y,r}$ can be determined from Eqn (10) with X' equal to $\frac{X}{N_v}$, i.e.,

$$K_{y,r} = \frac{(2\sigma^2)^r (r-1)!}{[\sqrt{1+2\gamma^2}+1]^r - [\sqrt{1+2\gamma^2}-1]^r} \times \qquad (33)$$

$$\left[1 + r\frac{X}{N_v} \sqrt{\frac{[(1+2\gamma^2)^{\frac{1}{2}}+1]^r - [(1+2\gamma^2)^{\frac{1}{2}}-1]^r}{[(1+2\gamma^2)^{\frac{1}{2}}+1]^r + [(1+2\gamma^2)^{\frac{1}{2}}-1]^r}} \; (1+2\gamma^2)^{\frac{1}{4}} \right]$$

Once the probability density function $f_z(z)$ is determined, the cumulative distribution function $F_z(z_T)$ can be found by integrating $f_z(z_T)$ in Eqn (30) from $-\infty$ to z_T. Hence,

$$F_Z(z_T) \simeq \Big[P(z') - \frac{C_1}{6}\phi^{(2)}(z') + \frac{C_2}{24}\phi^{(3)}(z') + \frac{C_1^2}{72}\phi^{(5)}(z') - \frac{C_3}{120}\phi^{(4)}(z') - \frac{C_1C_2}{144}\phi^{(6)}(z') - \frac{C_1^3}{1296}\phi^{(8)}(z') + \ldots\ldots \Big] \tag{34}$$

where

$$z' = \frac{\sigma z_T - NK_{y,1}}{\sqrt{NK_{y,2}}} \tag{35}$$

$$P(z') = \int_{-\infty}^{z'} \frac{1}{\sqrt{2\pi}} \exp\left[-\frac{z^2}{2} \right] dz = 0.5 \operatorname{erf}\left[\frac{z'}{\sqrt{2}} \right] \tag{36}$$

The probability of false alarm P_{fa} and the probability of detection P_d for a normalized threshold voltage of z_T can then be determined by taking the complement of Eqn (34), i.e.,

$$P_{fa} = 1 - F_{Z,0}(z_T) \tag{37}$$

$$P_d = 1 - F_{Z,1}(z_T) \tag{38}$$

where $F_{z,o}(z_T)$ denotes the cumulative distribution for the hypothesis that the target is absent while $F_{z,1}(z_T)$ denotes the cumulative distribution for the hypothesis that the target is present.

The receiver operating characteristics is then obtained by plotting the probability of detection versus the probability of false alarm with X, γ, and N as parameters.

It is obvious from the above expressions that the process involved in the computation of the output probability density function $f(z)$ and the receiver operating characteristics is numerically tedious. However, the steps involved are straight forward and can be easily programmed for execution in a digital computer. As part of this thesis, routines in PC-MATLAB have been written to compute the cumulants, the probability density functions, and the associated receiver operating characteristics. These routines are listed in Appendix B.

Using these routines, the effect of insufficient video bandwdith on the the detection statistics of the Gaussian square-law system can be investigated for various values of γ, input signal-to-noise ratio, and N. This is illustrated in Figure 3 to Figure 5.

Figure 3 compares the output probability density functions obtained for a finite video bandwidth equal to a quarter of the IF bandwidth ($\gamma=2$) against the corresponding density

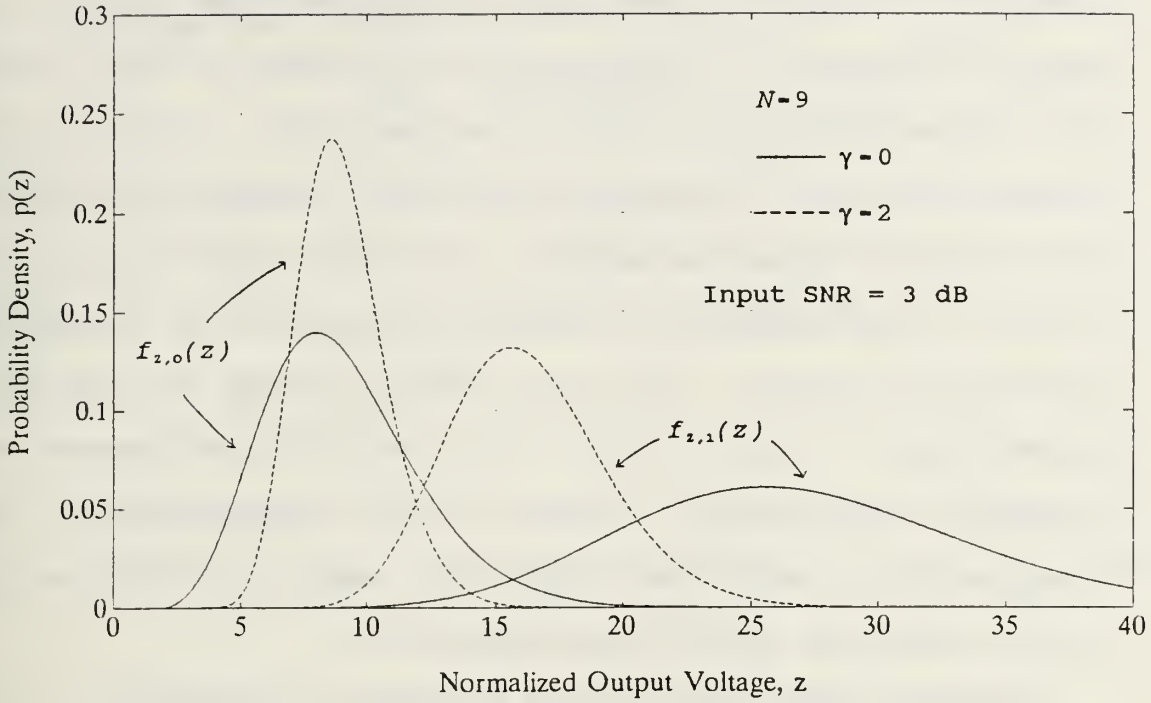

Figure 3. Gaussian square law system output probability density function.

functions when the video bandwidth is infinite ($\gamma = 0$). The output probability density functions corresponding to the absence and presence of a target are respectively denoted by $f_{z,0}(z)$ and $f_{z,1}(z)$. For this illustration, the number of video samples integrated, N, is chosen to be nine and the signal-to-noise ratio in the IF range bin is assumed to be 3 dB when there is a target return. The choice of these parameters is in part to facilitate comparison with Marcum's plots [Fig.4, Ref. 2] which assumed infinite video bandwidth. Accordingly, the plots in Figure 3 for $\gamma = 0$ are found to be in agreement with Marcum's results which serves as a validation of the

method and routines developed to compute the probability density functions. Graphically, the effect of the finite video bandwidth is observed to be two-fold. Firstly, the variance of $f_{z,0}(z)$ is reduced vis-a-vis the density function for infinite video bandwidth. Secondly, the variance of $f_{z,1}(z)$ is also reduced but this is accompanied by a leftward shift of the mode. The net result is that for the same probability of false alarm, the detection performance has degraded considerably. This is the consequence of the integration of additional noise-only samples induced by the finite bandwidth of the video amplifier.

Figure 4 shows the receiver operating characteristics for $\gamma = 0$ and $\gamma = 1$. The number of video samples integrated N is equal to 64. For a given signal-to-noise ratio and probability of false alarm, it can be seen that the probability of detection achievable for the system with the finite video bandwidth ($\gamma = 1$) is poorer than the system with the theoretical reference of infinite video bandwidth. Conversely, the system with the finite video bandwidth will require a higher signal-to-noise ratio to have the same performance as the system with infinite video bandwidth. This is illustrated in Figure 5. For a probability of false alarm and probability of detection equal to 10^{-7} and 0.95 respectively, a system with infinite video bandwidth will require an input signal-to-noise ratio of 0 dB. To achieve

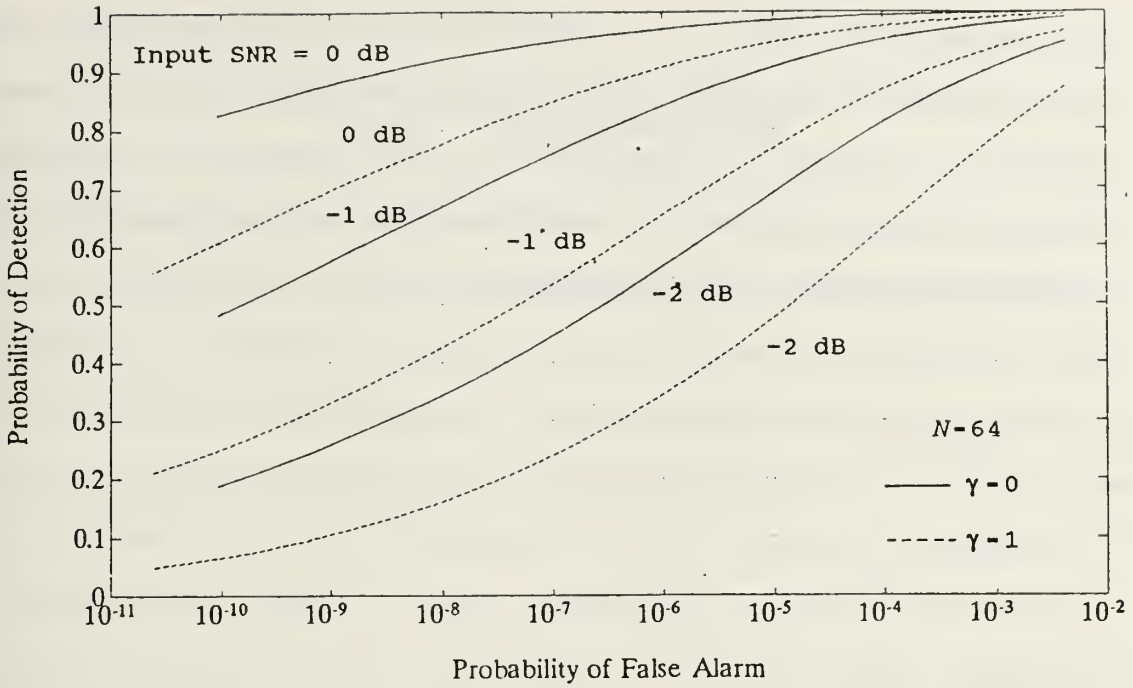

Figure 4. Gaussian square-law system operating characteristics

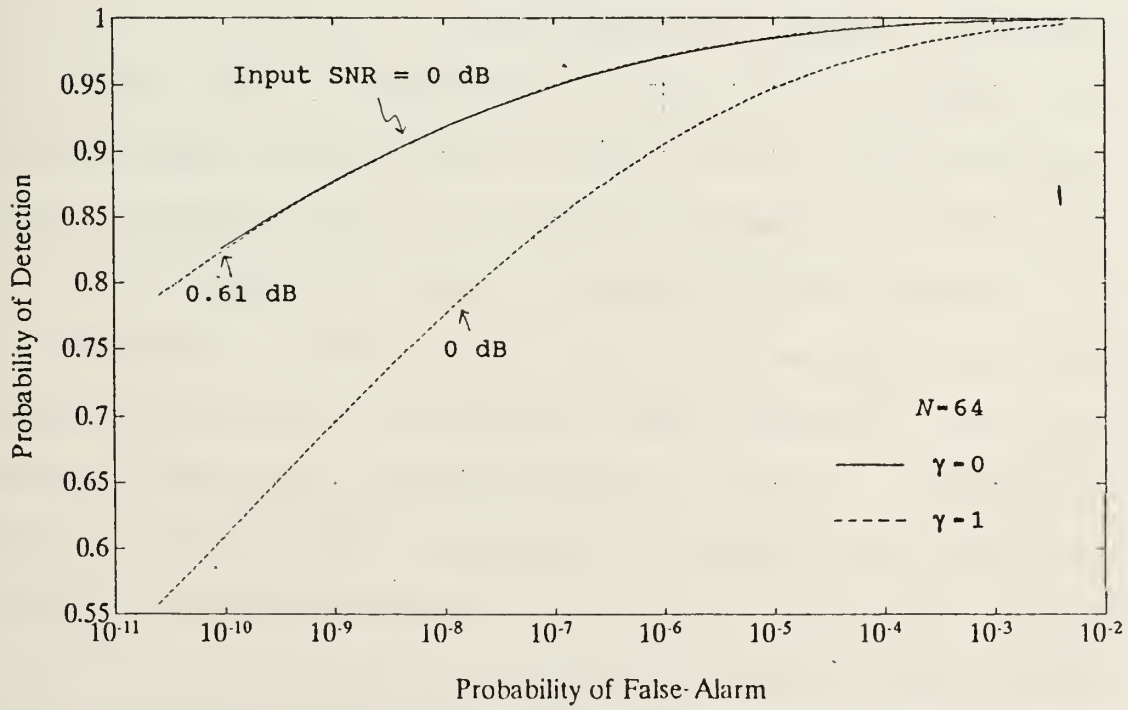

Figure 5. Gaussian square-law system operating characteristics.

the same performance, the system with a video bandwidth that is half the IF bandwidth will require an input signal-to-noise ratio of 0.61 dB. From Eqn (1), this implies a collapsing loss of 0.61 dB that is attributable to the 'insufficient' bandwidth of the video amplifier.

III. COLLAPSING RATIO

The statistical analysis in the preceding section provides the theoretical background and insight concerning bandwidth effects of a Gaussian-shaped video filter on the performance of the square-law detector. The analysis has also shown how sets of receiver operating characteristics such as those shown in Figure 4 can be generated using a digital computer to determine the input signal-to-noise required to attain a desired probability of detection for a specified probability of false alarm and a given IF bandwidth to video bandwidth ratio. While such an approach is feasible, it is more convenient in practice to follow Marcum's approach, using the collapsing ratio ρ defined in Eqn (2) to determine the required input signal-to-noise ratio. This is because the use of the collapsing ratio will obviate the need to generate sets of receiver operating characteristics for each value of γ. As explained in Section I, only the receiver operating characteristics for an infinite video bandwidth ($\gamma = 0$) are necessary once the collapsing ratio is known. Furthermore, there are usually other sources of collapsing loss apart from insufficient video bandwidth in practical systems. In such cases, the formulation of the collapsing ratio induced by each source will facilitate computation of the overall collapsing

loss. A general treatment of the problem of multiple sources of collapsing loss can be found in Meyer [Ref. 4] and Barton [Ref 5]. It is however beyond the scope of this report. In this section, the aim is to formulate the collapsing ratio associated with insufficient video bandwidth for the Gaussian square-law system and to compare the result with Barton's formula for the collapsing ratio in Eqn (5).

From Marcum's definition of the collapsing ratio,

$$\rho = \frac{M + N}{N} \tag{39}$$

where M is the number of additional noise-only samples integrated along with the N signal-plus-noise samples.

From the analysis of Section II, the number of additional noise-only samples integrated for every signal-plus-noise sample integrated in the Gaussian square law system is equal to N_v-*1* where N_v is given by Eqn (26). It follows that if the number of signal-plus-noise samples integrated is equal to N, then

$$M = N \times (N_v - 1) \tag{40}$$

and

$$\rho_G = \frac{N(N_v - 1) + N}{N} = N_v \tag{41}$$

Hence, the collapsing ratio caused by insufficient video bandwidth in the Gaussian square-law system is equal to the equivalent number of independent IF samples N_v averaged by the video filter.

The subscript 'G' has been used to denote that the collapsing ratio ρ_G given in Eqn (41) is caused by insufficient video bandwidth in a Gaussian square-law system. It is also used to distinguish from Barton's formula for the collapsing ratio:

$$\rho_B = \frac{B_{if} + 2B_v}{2B_v} = 1 + \gamma \qquad (42)$$

For convenience, ρ_G and ρ_B shall respectively be referred as the Gaussian system formula and Barton's formula in the context of collapsing ratios caused by video bandwidth. As pointed out in Section I, Barton's formula models the actual filters with ideal rectangular shaped filters having bandwidths equal to the noise-equivalent bandwidths of the actual filters. A comparison of the two formulae will provide a relative measure of the accuracy of Barton's formula in modelling systems that approximate the Gaussian square-law system.

Figure 6 plots the collapsing ratio formulae ρ_G and ρ_B as a function of the ratio γ of IF bandwidth to twice the video bandwidth. The plot obtained by applying Barton's formula is

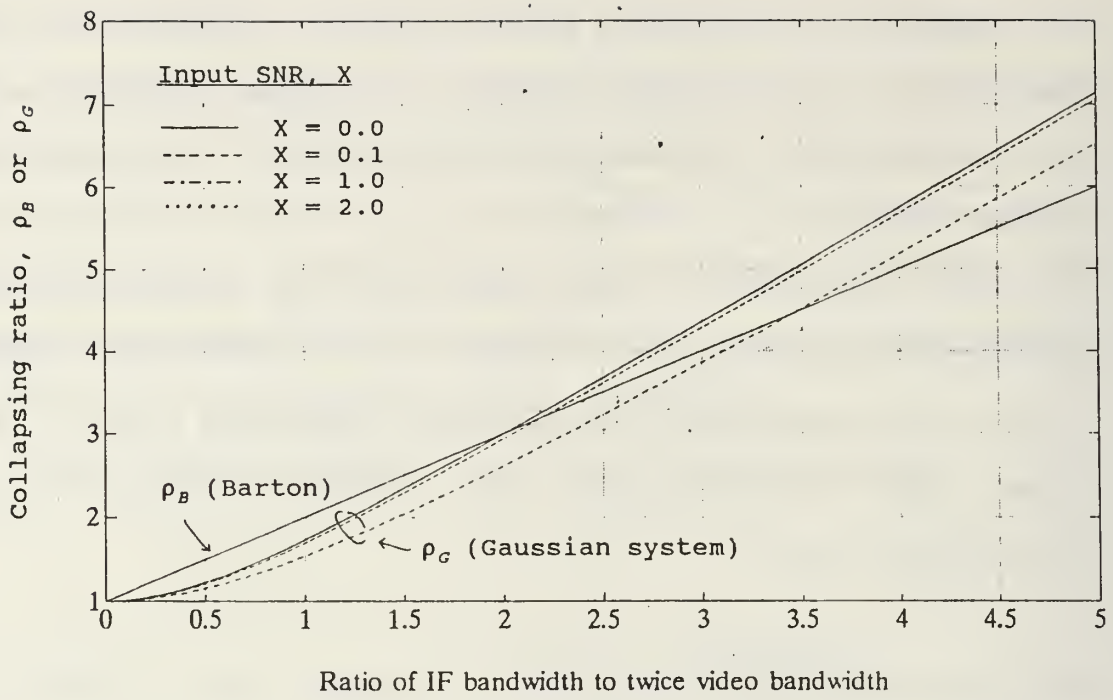

Figure 6. Collapsing ratio due to insufficient video bandwidth.

indicated in the figure. As expected from Eqn (42), it is a linear plot and is independent of input signal-to-noise ratio. All the other curves are obtained by applying the Gaussian system formula for input signal-to-noise ratios of 0, 0.1, 1, and 2. It is is seen that ρ_G is a function of the input signal-to-noise ratio X. For the same γ, the collapsing ratio given by ρ_G decreases as the signal-to-noise ratio increases. This dependency complicates the method of using the collapsing ratio to determine the required signal-to-noise ratio to attain a specified probability of detection and

probability of false alarm since the collapsing ratio is itself a function of the signal-to-noise ratio. For very small signal-to-noise ratios ($X \ll 1$), the collapsing ratio ρ_G can be approximated as

$$\rho_G = \sqrt{1 + 2\gamma^2} \tag{43}$$

which is independent of the input signal-to-noise ratio.

The collapsing ratio given by Eqn (43) can be considered as the worst case situation for any given γ in the Gaussian square-law system. Taking $\rho_G = \sqrt{1+2\gamma^2}$ as the reference, it is seen that Barton's formula overestimates the collapsing ratio for γ less than two. In this region, the largest relative deviation is about 22.5% in the vicinity of $\gamma = 0.5$. For $\gamma > 2$, Barton's formula underestimates the collapsing ratio. For large γ, ρ_B/ρ_G approaches $1/\sqrt{2}$ so that Barton's formula underestimates the collapsing ratio by a factor of about $\sqrt{2}$ for very large γ.

The collapsing loss associated with each collapsing ratio can be determined by finding the incremental increase in signal-to-noise ratio required with respect to the signal-to-noise ratio required in the ideal case of infinite video bandwidth for the same detection performance. Marcum has found that the collapsing loss is a function of the number of signal-plus-noise samples integrated but varies only slightly

with the probability of detection P_d and probability of false alarm P_{fa} [Ref. 2]. His results for the collapsing loss as a function of the collapsing ratio γ and with N as a parameter is shown in Figure 7 for $P_d = 0.5$ and $P_{fa} = 10^{-10}$.

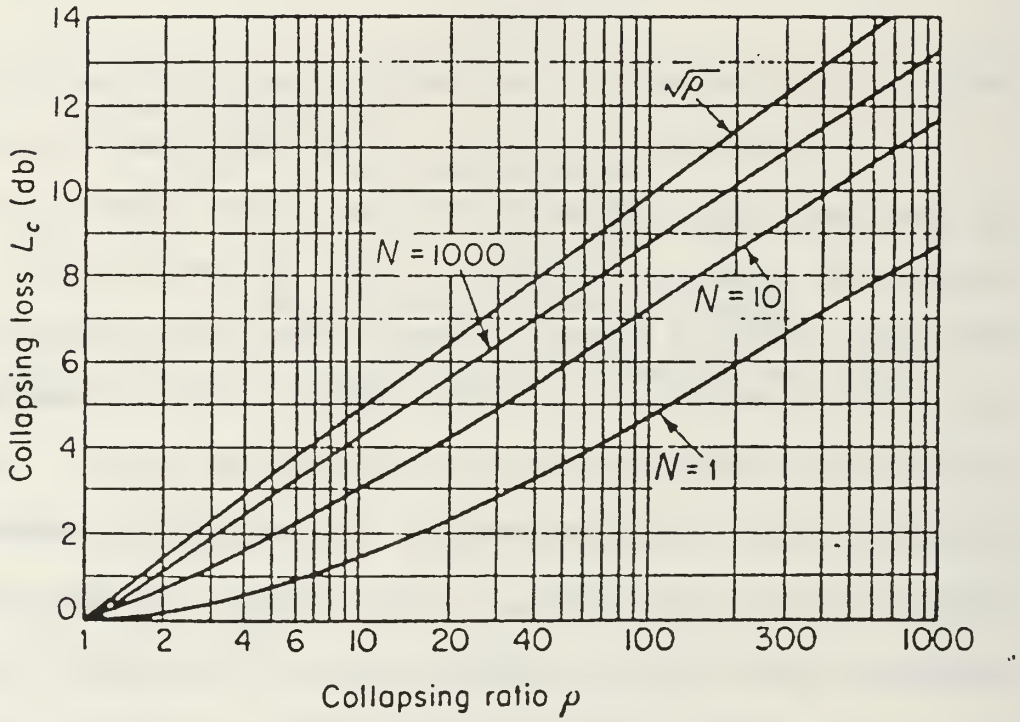

Figure 7. Collapsing loss vs. collapsing ratio for $P_d = 0.5$ and $P_{fa} = 10^{-10}$. (From Ref. 4)

Using Figure 7 and the respective equations for ρ_B and ρ_G, the collapsing losses predicted by the application of Barton's formula are compared against those deduced using the Gaussian system formula for selected values of γ in Table I and Table II. The collapsing loss associated with the use of Barton's

formula is denoted in the table by $L_{c,b}$ while that associated with the Gaussian system formula is denoted by $L_{c,g}$. Using $L_{c,g}$ as the reference, the difference between the two collapsing loss for a given γ is denoted by $\Delta L_{c,g}$. In Table I, the input signal-to-noise ratio X is assumed to be much less than one so that the collapsing ratio ρ_B can be taken to be equal to $\sqrt{1+2\gamma^2}$. A signal-to-noise ratio equal to one is assumed in Table II to provide a relative bound on the collapsing loss for signal-to-noise ratios between zero and one.

The comparison shows that for small signal-to-noise ratios, the collapsing loss predicted by Barton's collapsing ratio is within 0.3 dB of that deduced by the Gaussian system formula. If the signal-to-noise ratio is near or equal to one, Barton's formula overestimates the collapsing loss by about 0.4 dB for video bandwidths around half the IF bandwidth.

Typically, the number of pulses integrated in a search radar may range from thirty to forty. In such cases, the required single-pulse input signal-to-noise ratio is close to unity for reliable detection performance [Ref. 5]. From Table II, it follows that the collapsing loss will be overestimated by about 0.4 dB if Barton's formula is used in a Gaussian square-law system with a video bandwidth about half the IF bandwidth.

TABLE I. COMPARISON OF COLLAPSING LOSS.
BARTON'S FORMULA VS GAUSSIAN SYSTEM FORMULA.

Input SNR $X \ll 1$			Collapsing loss, L_c dB					
			N = 10			N = 1000		
γ	ρ_B	ρ_G	$L_{c,b}$	$L_{c,g}$	ΔL_c	$L_{c,b}$	$L_{c,g}$	ΔL_c
1.0	2.0	1.7	0.7	0.5	+0.2	1.1	0.8	+0.3
3.0	4.0	4.4	1.6	1.8	-0.2	2.5	2.8	-0.3
5.0	6.0	7.1	2.2	2.4	-0.2	3.3	3.6	-0.3

TABLE II. COMPARISON OF COLLAPSING LOSS.
BARTON'S FORMULA VS GAUSSIAN SYSTEM FORMULA.

Input SNR $X = 1$			Collapsing loss, L_c dB					
			N = 10			N = 1000		
γ	ρ_B	ρ_G	$L_{c,b}$	$L_{c,g}$	ΔL_c	$L_{c,b}$	$L_{c,g}$	ΔL_c
1.0	2.0	1.5	0.7	0.3	+0.4	1.1	0.6	0.5
2.0	3.0	2.6	1.2	1.0	+0.2	1.8	1.6	+0.2
5.0	6.0	6.5	2.2	2.3	-0.1	3.3	3.4	-0.1

IV. CONCLUSIONS

The effects of Gaussian-shaped IF and video filters on the performance of a square-law detector in pulsed radar applications employing post-detection integration have been analyzed in this paper.

Specifically, a formula for determining the number of additional noise-only samples integrated due to the finite bandwidth of the video filter has been derived. Emerson's formulation for the cumulants of the voltage probability density function at the output of the video filter has been used in this derivation.

The resultant cumulants of the probability density function at the output of the post-detection integrator are obtained. Based on these cumulants and Edgeworth's asymptotic expansion of the Gram-Charlier series to represent the density functions, MATLAB routines have been written to plot the receiver operating characteristics for various ratios of IF bandwidth to video bandwidth. The degradation in performance or collapsing loss can be observed and quantified from these operating characteristics as the video bandwidth is reduced relative to the IF video bandwidth.

Taking into account the Gaussian shape of the filters, the collapsing ratio is found to be equal to the equivalent

number N_v of independent IF samples averaged by the video filter. This is given by Eqn (25) which is a quadratic equation in N_v with signal-to-noise ratio and IF bandwidth to video bandwidth ratio as parameters. The collapsing ratios given by Eqn (25) and the associated collapsing loss are compared against those predicted by Barton's formula in Table I and II. The comparison shows that for typical signal-to-noise ratios close to 0 dB and video bandwidths about half the IF bandwidth, Barton's formula for the collapsing ratio results in an overestimation of the collapsing loss by about 0.4 dB.

APPENDIX A

MATHEMATICAL DERIVATION OF THE CUMULANTS

This appendix follows the method of Emerson [Ref. 7] in deriving a closed form expression for the cumulants of the probability density function $f_y(y)$ at the output of the Gaussian video filter shown in Figure A-1.

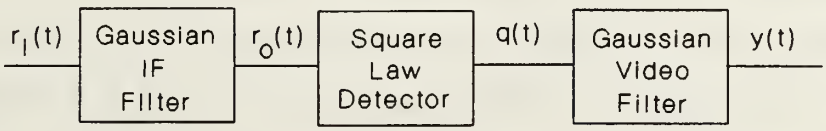

Figure A-1. Block diagram of the receiver.

The input to the system is a Gaussian random process given by:

$$r_i(t) = s(t) + n(t) \tag{A-1}$$

where

$$s(t) = \sqrt{2}\,A \cos \omega_o t \tag{A-2}$$

and n(t) is additive white Gaussian noise (AWGN) with a power spectral density equal to $\eta/2$.

The impulse response functions of the Gaussian-shaped IF filter and video filters are respectively defined by:

$$h_{if}(t) = 2(2\pi\beta^2)^{\frac{1}{2}} \exp[-(2\pi\beta)^2 \frac{t^2}{2}] \cos 2\pi f_o t \qquad \text{(A-3)}$$

and

$$h_v(t) = (2\pi\nu^2)^{\frac{1}{2}} \exp[-(2\pi\nu)^2 \frac{t^2}{2}] \qquad \text{(A-4)}$$

where β and ν are respectively the root-mean-square (rms) bandwidths of the IF and video filters.

The starting point in this derivation is the following general expression of the cumulants K_r obtained by Emerson for an arbitrary input signal contaminated by AWGN into a square-law detector with IF and video filters of arbitrary frequency response characteristics:

$$K_r = (\eta)^r \frac{(r-1)!}{2} \sum_{i-0}^{\infty} \lambda_i^r + (\eta)^{r-1} r! \sum_{i-0}^{\infty} \lambda_i^r s_i(t)^2 \qquad \text{(A-5)}$$

where

$$s_i(t) = \int_{-\infty}^{\infty} s(t-x)\, \phi_i(x)\, dx \qquad \text{(A-6)}$$

λ_i and $\phi_i(x)$ are respectively the eigenvalues and eigenfunctions defined by the integral equation:

$$\lambda_i \phi_i(x) = \int_{-\infty}^{\infty} g(x,y)\, \phi_i(y)\, dy \qquad \text{(A-7)}$$

The function $g(u,v)$ is called the system kernel and it is completely defined by the impulse response functions of the filters. In particular, it is defined by the following equation:

$$g(u,v) = \int_{-\infty}^{\infty} h_{if}(u-z)\, h_v(z)\, h_{if}(v-z)\, dz \qquad \text{(A-8)}$$

which can be expanded into the uniformly convergent bilinear Mercer series, i.e.,

$$g(u,v) = \sum_{i=0}^{\infty} \lambda_i \phi_i(u)\, \phi_i(v) \qquad \text{(A-9)}$$

To determine the cumulants for the Gaussian system shown in Figure A-1, the method of solution is to evaluate the system kernel using Eqn (A-8) and expressing it in a form that matches the Mercer series. The eigenvalues and eigenfunctions that satisfy the integral equation of Eqn (A-7) can then be identified. The cumulants can then be determined by using these eigenvalues and eigenfunctions to evaluate Eqn (A-5).

Thus using Eqn (A-8), the system kernel for the Gaussian system shown in Figure A-1 is given by

$$g(u,v) = \int_{-\infty}^{\infty} 2\sqrt{2\pi}\,\beta \exp\left[-(2\pi\beta)^2 \frac{(u-z)^2}{2}\right] \cos\omega_o(u-z)$$

$$\times \sqrt{2\pi}\,\nu \exp\left[-(2\pi\nu)^2 \frac{z^2}{2}\right]$$

$$\times 2\sqrt{2\pi}\,\beta \exp\left[-(2\pi\beta)^2 \frac{(v-z)^2}{2}\right] \cos\omega_o(v-z)$$

$$\times dz \qquad \text{(A-10)}$$

Now,

$$\cos\omega_o(u-z)\,\cos\omega_o(v-z) \qquad \text{(A-11)}$$

$$= \frac{1}{2}\cos\omega_o(u-v) +$$

$$\frac{1}{2}\left[\sin\omega_o(u+v)\,\sin 2\omega_o z + \sin\omega_o(u+v)\,\sin 2\omega_o z\right]$$

Substituting Eqn (A-11) into Eqn (A-10),

$$\Rightarrow \quad g(u,v) = 4\pi\beta^2\sqrt{2\pi}\,[g_1 + g_2] \qquad \text{(A-12)}$$

where

$$g_1 = \cos\omega_o(u-v) \int_{-\infty}^{\infty} \exp\left[-\left\{ \frac{(2\pi\beta)^2}{2} \left[(u-z)^2 + (v-z)^2 \right] + \frac{(2\pi\nu)^2}{2} z^2 \right\} \right] dz \qquad \text{(A-13)}$$

$$g_2 = \int_{-\infty}^{\infty} \cos\omega_o(u+v-2z) \exp\left[-\left\{ \frac{(2\pi\beta)^2}{2} \left[(u-z)^2 + (v-z)^2 \right] + \frac{(2\pi\nu)^2}{2} z^2 \right\} \right] dz \qquad \text{(A-14)}$$

The integral in Eqn (A-13) can be evaluated by completing the square in the exponent and casting the integrand into the form of the standard integral identity: [Ref. 12]

$$\int_{-\infty}^{\infty} \exp\left[-a^2 (x-m)^2 \right] dx = \frac{\sqrt{\pi}}{a} \qquad \text{(A-15)}$$

Thus completing the square,

$$g_1 = \cos\omega_o(u-v) \exp\left[-\frac{(2\pi\beta)^2}{2} \left\{ \frac{1+\gamma^2}{1+2\gamma^2} (u^2+v^2) - \frac{2\gamma^2 uv}{1+2\gamma^2} \right\} \right] \times \int_{-\infty}^{\infty} \exp\left\{ -\frac{2\pi^2\beta^2}{\gamma^2} (1+2\gamma^2) \left[z - \frac{\gamma^2}{1+2\gamma^2} (u+v) \right]^2 \right\} dz \qquad \text{(A-16)}$$

where

$$\gamma = \frac{\beta}{\nu} = \frac{B_{if}}{2B_v} \tag{A-17}$$

The symbols B_{if} and B_v in the above equation are respectively the noise equivalent bandwidths of the Gaussian IF and video filters.

Making use of Eqn (A-15) with $a = \frac{2\pi^2\beta^2}{\gamma^2}(1+2\gamma^2)$,

$$\therefore \quad g_1 = \cos\omega_o(u-v)\ \exp\left[-\frac{(2\pi\beta)^2}{4}\left\{\frac{1+\gamma^2}{1+2\gamma^2}(u^2+v^2) - \frac{2\gamma^2 uv}{1+2\gamma^2}\right\}\right] \times \frac{1}{\sqrt{2\pi}\,\nu\,(1+2\gamma^2)^{\frac{1}{2}}} \tag{A-18}$$

Now, consider the second term g_2 of the system kernel given in Eqn (A-12). By completing the square in the exponent as in the evaluation of g_1, it can be similarly shown that

$$g_2 = \exp\left[-\frac{(2\pi\beta)^2}{4}\left\{\frac{1+\gamma^2}{1+2\gamma^2}(u^2+v^2) - \frac{2\gamma^2 uv}{1+2\gamma^2}\right\}\right] \times \int_{-\infty}^{\infty} \cos\omega_o(u+v-2z)\ \exp[-a^2(z-m)^2]\ dz \tag{A-19}$$

where

$$a = \frac{\sqrt{2\pi\beta}}{\gamma}(1+2\gamma^2)^{\frac{1}{2}} \tag{A-20}$$

$$m = \frac{\gamma^2}{1+2\gamma^2}(u+v) \tag{A-21}$$

Now,

$$\int_{-\infty}^{\infty} \cos\omega_o(u+v-2z)\exp[-a^2(z-m)^2]\,dz \tag{A-22}$$

$$= \int_{-\infty}^{\infty} \cos\omega_o(u+v)\cos 2\omega_o z \exp[-a^2(z-m)^2]\,dz$$

$$+ \int_{-\infty}^{\infty} \sin\omega_o(u+v)\sin 2\omega_o z \exp[-a^2(z-m)^2]\,dz$$

Let $x = (z-m)$. Then,

$$\int_{-\infty}^{\infty} \cos\omega_o(u+v)\cos 2\omega_o z \exp[-a^2(z-m)^2]\,dz \tag{A-23}$$

$$= \cos\omega_o(u+v)\cos 2\omega_o m \int_{-\infty}^{\infty} \cos 2\omega_o x \exp[-a^2x^2]\,dx$$

$$- \cos\omega_o(u+v)\sin 2\omega_o m \int_{-\infty}^{\infty} \sin 2\omega_o x \exp[-a^2x^2]\,dx$$

From Eqn (679) of Ref. 12,

$$\int_{-\infty}^{\infty} \cos 2\omega_o x \exp[-a^2x^2]\,dx = \frac{\sqrt{\pi}}{a} \exp\left[-\frac{\omega_o^2}{a^2}\right] \tag{A-24}$$

$$\int_{-\infty}^{\infty} \sin 2\omega_o x \exp[-a^2x^2]\,dx = 0 \tag{A-25}$$

Hence,

$$\int_{-\infty}^{\infty} \cos\omega_o(u+v)\cos 2\omega_o z \exp[-a^2(z-m)^2]\, dz \qquad \text{(A-26)}$$

$$= \cos\omega_o(u+v)\cos 2\omega_o m \frac{\sqrt{\pi}}{a}\exp\left[-\frac{\omega_o^2}{a^2}\right]$$

The second integral in Eqn (A-22) can be similarly evaluated to give the following result:

$$\int_{-\infty}^{\infty} \sin\omega_o(u+v)\sin 2\omega_o z \exp[-a^2(z-m)^2]\, dz \qquad \text{(A-27)}$$

$$= \sin\omega_o(u+v)\sin 2\omega_o m \frac{\sqrt{\pi}}{a}\exp\left[-\frac{\omega_o^2}{a^2}\right]$$

Using the results of Eqn (A-22), Eqn (A-26), and Eqn (A-27) to evaluate Eqn (A-19), it can be shown that

$$g_2 = \exp\left[-\frac{(2\pi\beta)^2}{4}\left\{\frac{1+\gamma^2}{1+2\gamma^2}(u^2+v^2) - \frac{2\gamma^2 uv}{1+2\gamma^2}\right\}\right] \qquad \text{(A-28)}$$

$$\times \exp\left[-\frac{\omega_o^2}{2\pi^2\beta^2(1+2\gamma^2)}\right] \frac{\cos\left\{\omega_o(u+v)\frac{1+\gamma^2}{1+2\gamma^2}\right\}}{\sqrt{2\pi}\,\nu\,(1+2\gamma^2)^{\frac{1}{2}}}$$

Comparing Eqn (A-28) with Eqn (A-18), it is obvious that if $\omega_o > 2\pi\beta$, then g_2 will be small and negligible compared to

g_1. Hence, neglecting the contribution from g_2, the system kernel given in Eqn (A-12) becomes

$$g(u,v) = \frac{4\pi\beta^2 \cos\omega_o(u-v)}{\sqrt{1+2\gamma^2}} \times \exp\left[-\frac{(2\pi\beta)^2}{2} \left\{ \frac{1+\gamma^2}{1+2\gamma^2}(u^2+v^2) - \frac{2\gamma^2 uv}{1+2\gamma^2} \right\} \right] \quad \text{(A-29)}$$

Using the following substitutions,

$$u = \frac{(1+2\gamma^2)^{\frac{1}{4}}}{2\pi\beta} x \quad \text{(A-30)}$$

$$v = \frac{(1+2\gamma^2)^{\frac{1}{4}}}{2\pi\beta} y \quad \text{(A-31)}$$

$$t = \frac{\sqrt{1+2\gamma^2}-1}{\sqrt{1+2\gamma^2}+1} \quad \text{(A-32)}$$

Eqn (29) can be transformed into the following form suitable for the application of Mehler's formula:

$$g(u,v) = [\cos\omega_o u \cos\omega_o v + \sin\omega_o u \sin\omega_o v] \times \frac{4\pi\beta^2}{\sqrt{1+2\gamma^2}} \exp\left[-\frac{x^2+y^2}{2} \right] \exp\left[-\frac{t^2(x^2+y^2) - 2txy}{1-t^2} \right] \quad \text{(A-33)}$$

Using Mehler's formula,

$$\exp\left[-\frac{t^2(x^2+y2) - 2txy}{1-t^2} \right] = \sqrt{1-t^2} \sum_{i=0}^{\infty} H_i(x) H_i(y) \frac{t^i}{i!\,2^i} \quad \text{(A-34)}$$

where $H_i(x)$ is the Hermite polynomial defined by

$$H_i(x) = (-1)^i \exp[x^2] \frac{d^j}{dx^j} \exp[-x^2] \tag{A-35}$$

From Eqn (A-30) and Eqn (A-31),

$$x = \frac{2\pi\beta u}{(1+2\gamma^2)^{\frac{1}{4}}} \tag{A-36}$$

$$y = \frac{2\pi\beta v}{(1+2\gamma^2)^{\frac{1}{4}}} \tag{A-37}$$

Substituting the above equations into Eqn (A-33),

$$\therefore \quad g(u,v) = g_c(u,v) + g_s(u,v) \tag{A-38}$$

where

$$g_c(u,v) = \frac{2\beta\sqrt{\pi}}{1+\sqrt{1+2\gamma^2}} \left[\frac{\sqrt{1+2\gamma^2}-1}{\sqrt{1+2\gamma^2}+1} \right]^i \tag{A-39}$$

$$\times \frac{\sqrt{4\pi\beta} \exp\left[-\frac{(2\pi\beta)^2}{\sqrt{1+2\gamma^2}} \frac{u^2}{2} \right] \cos\omega_o u}{\left[2^i i! \sqrt{\pi} (1+2\gamma^2)^{\frac{1}{4}} \right]^{\frac{1}{2}}}$$

$$\times \frac{\sqrt{4\pi\beta} \exp\left[-\frac{(2\pi\beta)^2}{\sqrt{1+2\gamma^2}} \frac{v^2}{2} \right] \cos\omega_o v}{\left[2^i i! \sqrt{\pi} (1+2\gamma^2)^{\frac{1}{4}} \right]^{\frac{1}{2}}}$$

$$\times \sum_{i=0}^{\infty} H_i\left[\frac{2\pi\beta u}{(1+2\gamma^2)^{\frac{1}{4}}} \right] H_i\left[\frac{2\pi\beta v}{(1+2\gamma^2)^{\frac{1}{4}}} \right]$$

$$g_s(u,v) = \frac{2\beta\sqrt{\pi}}{1+\sqrt{1+2\gamma^2}} \left[\frac{\sqrt{1+2\gamma^2}-1}{\sqrt{1+2\gamma^2}+1} \right]^i \qquad \text{(A-40)}$$

$$\times \frac{\sqrt{4\pi\beta} \exp\left[-\frac{(2pe\beta)^2}{\sqrt{1+2\gamma^2}} \frac{u^2}{2} \right] \cos\omega_o u}{\left[2^i i! \sqrt{\pi} (1+2\gamma^2)^{\frac{1}{4}} \right]^{\frac{1}{2}}}$$

$$\times \frac{\sqrt{4\pi\beta} \exp\left[-\frac{(2\pi\beta)^2}{\sqrt{1+2\gamma^2}} \frac{v^2}{2} \right] \sin\omega_o v}{\left[2^i i! \sqrt{\pi} (1+2\gamma^2)^{\frac{1}{4}} \right]^{\frac{1}{2}}}$$

$$\times \sum_{i=0}^{\infty} H_i\left[\frac{2\pi\beta u}{(1+2\gamma^2)^{\frac{1}{4}}} \right] H_i\left[\frac{2\pi\beta v}{(1+2\gamma^2)^{\frac{1}{4}}} \right]$$

By comparing Eqn (A-38) against the Mercer series expansion of the system kernel

$$g_c(u,v) = \sum_{i=0}^{\infty} \lambda_{c,i} \phi_{c,i}(u) \phi_{c,i}(v) \qquad \text{(A-41)}$$

the eigenvalues and eigenfunctions can be deduced to be

$$\lambda_{c,i} = \frac{2\beta\sqrt{\pi}}{1+\sqrt{1+2\gamma^2}} \left[\frac{\sqrt{1+2\gamma^2}-1}{\sqrt{1+2\gamma^2}+1} \right]^i \qquad \text{(A-42)}$$

$$\phi_{c,i}(u) = \frac{\sqrt{4\pi\beta} \exp\left[-\frac{(2\pi\beta)^2}{\sqrt{1+2\gamma^2}} \frac{u^2}{2} \right] H_i\left[\frac{2\pi\beta u}{(1+2\gamma^2)^{\frac{1}{4}}} \right] \cos\omega_o u}{\left[2^i i! \sqrt{\pi} (1+2\gamma^2)^{\frac{1}{4}} \right]^{\frac{1}{2}}}$$

(A-43)

Similarly, it can be shown that

$$\lambda_{s,i} = \lambda_{c,i} \tag{A-44}$$

$$\phi_{s,i}(u) = \frac{\sqrt{4\pi\beta}\,\exp\left[-\frac{(2\pi\beta)^2}{\sqrt{1+2\gamma^2}}\,\frac{u^2}{2}\right] H_i\left[\frac{2\pi\beta u}{(1+2\gamma^2)^{\frac{1}{4}}}\right] \sin\omega_o u}{\left[\,2^i i!\,\sqrt{\pi}\,(1+2\gamma^2)^{\frac{1}{4}}\,\right]^{\frac{1}{2}}} \tag{A-45}$$

Hence, from Eqn (A-42) and Eqn (A-44),

$$\sum_{i=0}^{\infty} (\lambda_{c,i})^r = \sum_{i=0}^{\infty} (\lambda_{s,i})^r \tag{A-46}$$

$$= \frac{(2\beta\sqrt{\pi})^r}{(1+\sqrt{1+2\gamma^2})^r} \sum_{i=0}^{\infty} \left[\frac{\sqrt{1+2\gamma^2}-1}{\sqrt{1+2\gamma^2}+1}\right]^{ri}$$

Now, $\sum_{i=0}^{\infty} x^i = \frac{1}{1-x}$ for $|x| < 1$.

Hence,

$$\sum_{i=0}^{\infty} (\lambda_{c,i})^r = \sum_{i=0}^{\infty} (\lambda_{s,i})^r = \frac{(2\beta\sqrt{\pi})^r}{(\sqrt{1+2\gamma^2}+1)^r - (\sqrt{1+2\gamma^2}-1)^r} \tag{A-47}$$

$$\sum_{i=0}^{\infty} (\lambda_i)^r = \sum_{i=0}^{\infty} (\lambda_{c,i})^r + \sum_{i=0}^{\infty} (\lambda_{s,i})^r$$

$$= \frac{2\,(2\beta\sqrt{\pi})^r}{(\sqrt{1+2\gamma^2}+1)^r - (\sqrt{1+2\gamma^2}-1)^r} \tag{A-48}$$

From Eqn (A-12) and Eqn (A-45),

$$s_{c,i}(t) = \sqrt{2}A \int_{-\infty}^{\infty} \cos\omega_o(t-u)\ \phi_{c,i}(u)\ du$$

$$= \frac{\sqrt{2}A\ (4\pi\beta)^{\frac{1}{2}}}{[\ 2^i i!\sqrt{\pi}\ (1+2\gamma^2)^{\frac{1}{4}}\ ]^{\frac{1}{2}}} \qquad \text{(A-49)}$$

$$\times \int_{-\infty}^{\infty} \exp(-\alpha^2\frac{u^2}{2})\ H_i(\alpha u)\ \cos\omega_o u\ \cos\omega_o(t-u)\ \ du$$

where

$$\alpha = \frac{2\pi\beta}{(1+2\gamma^2)^{\frac{1}{4}}} \qquad \text{(A-50)}$$

$$\cos\omega_o u\ \cos\omega_o(t-u) = \frac{1}{2}\cos\omega_o t + \frac{1}{2}\cos(2\omega_o u + t) \qquad \text{(A-51)}$$

For $\omega_o \gg 2\pi\beta$, the residue from the high frequency component in Eqn (A-51) can be neglected in the integration of Eqn (A-49). Hence,

$$s_{c,i}(t) = \frac{\sqrt{2}A(4\pi\beta)^{\frac{1}{2}}}{[\ 2^i i!\sqrt{\pi}\ (1+2\gamma^2)^{\frac{1}{4}}\ ]^{\frac{1}{2}}} \frac{\cos\omega_o t}{2} \qquad \text{(A-52)}$$

$$\times \int_{-\infty}^{\infty} \exp(-\alpha^2\frac{u^2}{2})\ H_i(\alpha u)\ du$$

The following integral identities derived in Ref. 13 are useful in evaluating (A-52):

$$\int_{-\infty}^{\infty} \exp(-x^2)\, H_{2n+1}(\sqrt{2}x)\, dx = 0 \qquad \text{(A-53)}$$

$$\int_{-\infty}^{\infty} \exp(-x^2)\, H_{2n}(\sqrt{2}x)\, dx = \frac{(2n)!\sqrt{\pi}}{n!} \qquad \text{(A-54)}$$

Let $\alpha^2 \frac{u^2}{2} = x^2$ (A-55)

Then $\alpha u = \sqrt{2}x$ and $du = \frac{\sqrt{2}}{\alpha} dx$.

Using the above substitution, Eqn (A-53) and Eqn (A-54)

$$\therefore \int_{-\infty}^{\infty} \exp(-\alpha^2 \frac{u^2}{2})\, H_i(\alpha u)\, du$$

$$= \frac{\sqrt{2}\,(1+2\gamma^2)^{\frac{1}{4}}}{2\pi\beta} \int_{-\infty}^{\infty} \exp(-x^2)\, H_i(\sqrt{2}x)\, dx$$

$$= \begin{cases} \dfrac{\sqrt{2\pi}\,(1+2\gamma^2)^{\frac{1}{4}}}{2\pi\beta} \dfrac{i!}{(\frac{i}{2})!} & \text{for } i \text{ even} \\ 0 & \text{for } i \text{ odd} \end{cases} \qquad \text{(A-56)}$$

Hence, using the result of Eqn (A-56) to evaluate Eqn (A-52)

$$s_{c,i}(t) = \begin{cases} \left(\frac{\sqrt{2A^2}}{2\beta\sqrt{\pi}}\right)^{\frac{1}{2}} (1+2\gamma^2)^{\frac{1}{8}} \frac{(i!)^{\frac{1}{2}}}{2^{\frac{i}{2}}\left(\frac{i}{2}\right)!} \cos\omega_o t & \text{for } i \text{ even.} \\ 0 & \text{for } i \text{ odd.} \end{cases} \tag{A-57}$$

A similar result is obtained for $s_{s,i}(t)$ except that the $\cos\omega_o t$ term in Eqn (A-57) is replaced by a $\sin\omega_o t$ term.

Using Eqn (A-40) and Eqn (A-55), it can be shown that

$$\sum_{-\infty}^{\infty} (\lambda_{c,i})^r s_{c,i}^2(t) = \frac{2A^2 (2\beta\sqrt{\pi})^{r-1}}{(1+\sqrt{1+2\gamma^2})^r} (1+2\gamma^2)^{\frac{1}{4}} \cos^2\omega_o t \times \sum_{-\infty}^{\infty} \left[\frac{\sqrt{1+2\gamma^2}-1}{\sqrt{1+2\gamma^2}+1}\right]^{2ri} \frac{(2i)!}{2^{2i}(i!)^2} \tag{A-58}$$

$$\text{Let} \quad \left[\frac{\sqrt{1+2\gamma^2}-1}{\sqrt{1+2\gamma^2}+1}\right]^{2r} = x \tag{A-59}$$

From Ref. 12,

$$\sum_{i=0}^{\infty} x^i \frac{(2i)!}{2^{2i}(i!)^2} = 1 + \frac{1}{2}x + \frac{\frac{1}{2}\left(\frac{1}{2}+1\right)x^2}{2!} + \ldots. = (1-x)^{-\frac{1}{2}} \tag{A-60}$$

Hence, using this result to evaluate Eqn (A-58) gives

$$\sum_{i=0}^{\infty} (\lambda_{c,i})^r s_{c,i}^2(t) = \frac{2A^2(2\beta\sqrt{\pi})^{r-1}(1+2\gamma^2)^{\frac{1}{4}}}{[(\sqrt{1+2\gamma^2}+1)^{2r}-(\sqrt{1+2\gamma^2}-1)^{2r}]^{\frac{1}{2}}} \cos^2\omega_o t$$

(A-61)

Similarly, it can be shown that

$$\sum_{i=0}^{\infty} (\lambda_{s,i})^r s_{s,i}^2(t) = \frac{2A^2(2\beta\sqrt{\pi})^{r-1}(1+2\gamma^2)^{\frac{1}{4}}}{[(\sqrt{1+2\gamma^2}+1)^{2r}-(\sqrt{1+2\gamma^2}-1)^{2r}]^{\frac{1}{2}}} \sin^2\omega_o t$$

(A-62)

Hence,

$$\sum_{i=0}^{\infty} (\lambda_i)^r s_i^2(t) = \sum_{i=o}^{\infty} (\lambda_{c,i})^r s_{c,i}^2(t) + \sum_{i=0}^{\infty} (\lambda_{s,i})^r s_{s,i}^2(t)$$

$$= \frac{2A^2(2\beta\sqrt{\pi})^{r-1}(1+2\gamma^2)^{\frac{1}{4}}}{[(\sqrt{1+2\gamma^2}+1)^{2r}-(\sqrt{1+2\gamma^2}-1)^{2r}]^{\frac{1}{2}}}$$

(A-63)

From Eqn (A-5) and the results of Eqn (A-48) and Eqn (A-63),

$$\therefore \quad K_r = (\eta)^r \frac{(r-1)!}{2} \sum_{i=0}^{\infty} (\lambda_i)^r + (\eta)^{r-1} r! \sum_{i=0}^{\infty} (\lambda_i)^r s_i^2(t)$$

$$= \frac{(2\eta\beta\sqrt{\pi})^r (r-1)!}{(\sqrt{1+2\gamma^2}+1)^r - (\sqrt{1+2\gamma^2}-1)^r} \times$$

$$\left[1 + r\frac{A^2}{\eta\beta\sqrt{\pi}} \sqrt{\frac{(\sqrt{1+2\gamma^2}+1)^r - (\sqrt{1+2\gamma^2}-1)^r}{[(\sqrt{1+2\gamma^2}+1)^r - (\sqrt{1+2\gamma^2}-1)^r]^{\frac{1}{2}}}} \right.$$

$$\left. \times \quad (1+2\gamma^2)^{\frac{1}{4}} \right] \qquad \text{(A-64)}$$

Now, it can be shown that the IF noise bandwidth B_{if} is equal to $\beta\sqrt{\pi}$. It follows that the total average power into the detector is given by

$$\sigma^2 = \eta\beta\sqrt{\pi} \qquad \text{(A-65)}$$

Hence,

$$K_r = \frac{(2\sigma^2)^r (r-1)!}{(\sqrt{1+2\gamma^2}+1)^r - (\sqrt{1+2\gamma^2}-1)^r} \times \qquad \text{(A-66)}$$

$$\left[1 + r\frac{A^2}{\sigma^2} \sqrt{\frac{(\sqrt{1+2\gamma^2}+1)^r - (\sqrt{1+2\gamma^2}-1)^r}{(\sqrt{1+2\gamma^2}+1)^r + (\sqrt{1+2\gamma^2}-1)^r}} \; (1+2\gamma^2)^{\frac{1}{4}} \right]$$

This equation which expresses the cumulants K_r in terms of the IF bandwidth to video bandwidth ratio γ and the input signal-to-noise ratio A^2/σ^2 concludes the mathematical derivation of this appendix.

APPENDIX B

MATLAB PROGRAMS FOR PLOTTING THE RECEIVER OPERATING CHARACTERISTICS

This appendix is a listing of the Matlab programs written as part of this thesis to plot the probability density functions and operating characteristics of the Gaussian square law system described in Section II. The programs are written as MATLAB M-Files. The following are respectively the filenames of the programs for plotting the probability density functions and operating characteristics:

1. *SQ2PDF.M*: This plots the probability density functions based on Eqn (29) which is an Edgeworth's asymptotic expansion of the Gram-Charlier series.

2. *SQ2ROC.M*: This plots the receiver operating characteristics based on Eqn (37) which is derived by integrating Eqn (29) from the threshold voltage to infinity.

These are *script* files which are run by invoking their filenames in the MATLAB operating environment. Both programs will prompt the user to enter the necessary input parameters prior to execution. In addition five *function* type M-Files are specifically created to facilitate programming and

execution of these *script* files. The filenames of these five *functions* and their purpose are:

1. *GCUMU.M*: This function computes the cumulants of the video filter output probability density funtion based on Eqn (10).
2. *GDFZ.M*: This function computes the probability density for given normalized values of the Gaussian square-law system output based on Eqn (29).
3. *UPFZ.M*: This function computes the probability of false alarm or probability of detection of the Gaussian square-law system for a specified threshold voltage. The computation is based on Eqn (37) and Eqn (38).
4. *GCR.M*: This function computes the collapsing ratio caused by the finite video bandwidth. It is based on Eqn (26).
5. *HMT.M*: This function computes the *m*th order Hermite polynomial for values of *m* less than or equal to 12.

The MATLAB source programs of the two *script* files and the five *function* files are provided in the remaining pages of this appendix.

1. SQ2PDF.M PROGRAM

```
% ============================================================
% This program computes and plots the pdf of a square law
% detector with Gaussian IF and video filters.  It will
% prompt the user to enter the following parameters:
%  a. Range and resolution of the x-axis for the plot.
%  b. SNR = input signal-to-noise ratio.  (Not in dB)
%  c. GAMMA = IF bandwidth to twice video bandwidth ratio.
%  d. N = Number of pulses to be integrated.
% In addition to the pdf plot for the specified GAMMA, the
% pdf plot for an infinite video bandwidth will automatically
% be plotted for comparison purposes.
% ------------------------------------------------------------
disp('The output pdf will be plotted as a function of the')
disp('normalized voltage, z.')
disp('Enter range and resolution of z to be plotted')
range = input('[zmin,zmax,zres] :  ')
N = input('Number of pulses to be integrated =  ')
SIGMA = input(Input noise rms voltage =   ')
SNR = [0 0]
GAMMA = [0 0]
ORDER = 4
SNR(2) = input('Enter input SNR:  ')
GAMMA(2) = input('Enter value of GAMMA:  ')
disp('Computing ...')
KY0 = []
KY1 = []
Z = range(1):range(3):range(2)
GAMMA0 = GAMMA(1)
for j = 1:2
  K = []
  SNRj = SNR(j)
  for r = 1:ORDER
    K(r) = gcumu(r,SIGMA,SNRj,GAMMA0)
  end
  if j == 1
    fZinf0 = gdpz(ORDER,N,Z,SIGMA,SNRj,GAMMA0)
  else
    fZinf1 = gdpz(ORDER,N,Z,SIGMA,SNRj,GAMMA0)
  end
end
GAMMAv = GAMMA(2)
SNRj = 0.0
for r = 1:ORDER+2
  KY0(r) = gcumu(r,SIGMA,SNRj,GAMMAv)
end
fZv0 = gdpz(ORDER,N,Z,SIGMA,SNRj,GAMMAv,KY0)
```

```
SNRj = SNR(2)
NPRIME = gcr(SNRj,GAMMAv)
SNRjbar = SNRj/NPRIME
for r = 1:Order+2
  KY1(r) = gcumu(r,SIGMA,SNRjbar,GAMMAv)
end
fZv1 = gdpz(ORDER,N,Z,SIGMA,SNRj,GAMMAv,KY1)
plot(Z,fZinf0,'-',Z,fZv0,'--',Z,fZinf1,'-',Z,fZv1,'--')
grid
xlabel('Normalized Output Voltage, z')
ylabel('Probability Density, f(z)')

% ========================================================
```

2. SQ2ROC.M PROGRAM

```
% ========================================================
% This program computes and plots the ROC data points for
% the Gaussian square law system.  It is programmed to provide
% accuracy up to the 4th grouping of Edgeworth's series.  To
% obtain any other order of accuracy, the local variable
% ORDER which is set to 4 and the function file gdfz.m must
% be modified accordingly.
% --------------------------------------------------------
disp('Choices:')
disp('1. Computing Pfa and Pd given a normalized threshold.')
disp('2. Pd vs Pfa curves.')
disp(' ')
CHOICE = input('Select one of the above:  ')
if CHOICE == 1
  ORDER = 4
  MORE = 1
  while MORE == 1
    N = input('Number of samples integrated =  ')
    SNR = input('Input SNR = ')
    SIGMA = input('Input rms noise voltage =  ')
    GAMMA = input('GAMMA =  ')
    VT = input('Normalized threshold voltage, VT =  ')
    disp('Computing ... ')
    for r = 1:ORDER+2
      KY0(r) = gcumu(r,SIGMA,0,GAMMA)
    end
    NPRIME = gcr(SNR,GAMMA)
    SNRjbar = SNRj/NPRIME
    for r = 1:ORDER+2
      KY1(r) = gcumu(r,SIGMA,SNRjbar,GAMMA)
    end
```

```
    Pfa = upfz(ORDER,N,VT,SIGMA,KY0,1)
    Pd =  upfz(ORDER,N,VT,SIGMA,KY1,1)
    disp('Do you wish to compute Pd vs Pfa for another VT?')
    MORE = input('Type 1 if YES, 0 if NO :  ')
  end
else
  N = input('Number of samples integrated =  ')
  GAMMA = input('GAMMA =  ')
  disp('Enter up to a maximum of 3 SNR values as elements of
[]')
  SNR = input('SNR [] =  ')
  SIGMA = input('Input rms noise voltage =  ')
  disp('Enter  range  &  resolution  of  z  to  be  used  in
computing')
  disp('the ROC.')
  range = input('[zmin,zmax,zres]')
  Z = range(1):range(3):range(2)
  for r = 1:ORDER+2
    KY0(r) = gcumu(r,SIGMA,0,GAMMA)
  end
  NPRIME = gcr(SNR,GAMMA)
  SNRjbar = SNR ./NPRIME
  for r = 1:ORDER+2
    KY1(r) = gcumu(r,SIGMA,SNRjbar,GAMMA)
  end
  Pfa(j,:) = upfz(ORDER,N,Z,SIGMA,KY0,0)
  Pd(j,:) = upfz(ORDER,N,Z,SIGMA,KY1,0)
  if length(SNR) == 1
    semilogx(Pfa,Pd,'-')
  elseif length(SNR) == 2
    semilogx(Pfa(1,:),Pd(1,:),Pfa(2,:),Pd(2,:))
  elseif length(SNR) == 3

semilogx(Pfa(1,:),Pd(1,:),Pfa(2,:),Pd(2,:),Pfa(3,:),Pd(3,:))
  end
  grid
  xlabel('Probability of False Alarm')
  ylabel('Probability of Detection')
end
%
=========================================================
```

3. GCUMU.M FUNCTION

```
function K = gcumu(r,SIGMA,SNR,GAMMA)
% ========================================================

% This function computes the rth cumulant of the output pdf
% of a square law detector with Gaussian IF and video filters.
% GAMMA is the ratio of the IF bandwidth to twice the video
% bandwidth.  SIGMA is the input rms noise.
% Reference:  Thesis Eqn (10).

%--------------------------------------------------------

G12 = 1 + 2*GAMMA^2
G12PR = (sqrt(G12) + 1)^r
G12MR = (sqrt(G12) - 1)^r
BN1 = (2 * SIGMA^2)^r
RM1 = r - 1
BN2 = fac(RM1)
BD1 = G12PR - G12MR
B = (BN1 * BN2)/BD1
CN1 = BD1
CD1 = G12PR + G12MR
C = sqrt(CN1/CD1)
K = B * (1 + r*SNR*G12^0.25)

% ========================================================
```

4. GDFZ.M FUNCTION

```
function fz  = gdfz(ORDER,N,Z,SIGMA,SNR,GAMMA,K)
% ========================================================

% This function computes the probability density for specified
% values of the Gaussian square law system normalized output,
Z.
% K is an array comprising the cumulants of the pdf.
% Reference: Thesis Eqn (29).

% --------------------------------------------------------

C = []
for j = 1:ORDER
  SUMn = 0.0
  SUMd = 0.0
  for m = 1:N
    SUMn = SUMn + K(m,j+2)/N
    SUMd = SUMd + K(m,j+2)/N
  C(j) = SUMn/(N^(j/2) * SUMd^((j+2)/2))
  end
fz = zeros(1,length(Z))
SUM = zeros(ORDER,length(Z))
X = (SIGMA*Z - N*K(1))/sqrt(N*K(2))
CONST = SIGMA/sqrt(N*K(2))
```

```
PSI0 = exp(-(Z .^2)/2)/sqrt(2*pi)
for j = 1:ORDER
  if j == 1
    SUM(1,:) = CONST * PSIO .*( 1 + hmt(Z,3) * C(1)/6 )
  elseif j == 2
    SUM(2,:) = CONST * PSIO .*( hmt(Z,4) * C(2)/24 + hmt(Z,6)
                    * (C(1))^2/72 )
  elseif j == 3
    SUM(3,:) = CONST * PSI0 .*( hmt(Z,5)*C(3)/12 + hmt(Z,7)*
                C(1)*C(2)/144 + hmt(Z,9)*(C(1))^3/1296 )
  elseif j == 4
    SUM(4,:) = CONST * PSI0 .*( hmt(Z,6)*C(4)/720 + hmt(Z,8)*
                ( (C(2))^2/1152 + C(1)*C(3)/720 ) + hmt(Z,10)*
                        ( C ( 1 ) ) ^ 2    *    C ( 2 ) / 1 7 2 8    +
hmt(Z,12)*((C(1))^4/31104)
  end
  fz = fz + SUM(j,:)
end
```

5. UPFZ.M FUNCTION

```
function UPTE = upfz(ORDER,N,Z,SIGMA,ERROR)
% ============================================================

% This function computes the Pfa or Pd of a Gaussian square
% law detector for a specified threshold normalized by the rms

% noise voltage at the input to the detector.  If the argument
% ERROR is set to 1, the function will return a two element
% row vector.  The second element indicates the order of
% accuracy of the Pfa or Pd value given by the first element.
% If ERROR is set to 0, then the function will return the
% the value of Pfa or Pd without any indication of the order
% of accuracy.
% Reference: Thesis Eqn (37) and Eqn (38).
%------------------------------------------------------------

C = []
for j = 1:ORDER
  SUMn = 0.o
  SUMd = 0.0
  for m = 1:N
    SUMn = SUMn + K(m,j+2)/N
    SUMd = SUMd + K(m,2)/N
  end
C(j) = SUMn/(N^(j/2) * SUMd^((j+2)/2))
end
ZZ = (SIGMA*Z - N*K(1))/sqrt(N*K(2))
PSI0 = exp(-ZZ .^2)/sqrt(2*pi)
ZM = ZZ/sqrt(2)
SUM1 = 0.5*erf(-INF,ZM,'high')
```

```
TERM1 = hmt(ZZ,2)*C(1)/6
TERM2 = hmt(ZZ,3)*C(2)/24 + hmt(ZZ,5)*C(1)^2/72
TERM3 = hmt(ZZ,4)*C(3)/120 + hmt(ZZ,6)*C(1)*C(2)/144 +
        hmt(ZZ,8)*C(1)^3/1296
TERM4 = hmt(ZZ,5)*C(4)/120 + hmt(ZZ,7)*C(2)^2/1152 +
        hmt(ZZ,7)*C(1)*C(3)/720 + hmt(ZZ,9)*C(1)^2*C(2)/1728
        hmt(ZZ,11)*C(1)^4/31104
SUM2 = PSI0 .*(TERM1 + TERM2 + TERM3 + TERM4)
if ERROR == 1
  UPTE(1) = 1 - (SUM1 - SUM2)
  UPTE(2) = PSI0 .*TERM4
else
  UPTE = 1 - (SUM1 - SUM2)
end
% ============================================================
```

6. GCR.M FUNCTION

```
function GRHO = gcr(SNR,GAMMA)
% ============================================================
% This function computes the collapsing ratio caused by
% insufficient video bandwidth in a Gaussian square law
% system.  GAMMA can be a vector but SNR must be single
valued.
% Note that GRHO is also the equivalent number of independent
% samples averaged by the video filter.
% Reference: Thesis Eqn (26).
% ------------------------------------------------------------
B12 = 1 + 2*GAMMA .^2
B11 = 1 + GAMMA .^2
B = 2*SNR*sqrt(B12 ./B11) - sqrt(B12)
C = -2*SNR*sqrt(B12)
GRHO = 0.5*(-b + sqrt(B .^2 - 4*C)
% ============================================================
```

7. HMT.M FUNCTION

```
function H = hmt(Z,m)
% ============================================================
% This function computes the mth order Hermite polynomial for
% values of m less than or equal to 12.
% ------------------------------------------------------------
if m == 0
  H = 1
elseif m == 1
  H = Z
```

```
elseif m == 2
  H = Z .^2 - 1
elseif m == 3
  H = Z .^3 - 3*Z
elseif m == 4
  H = Z .^4 - 6*Z .^2 + 3
elseif m == 5
  H = Z .^5 - 10*Z .^3 + 15*Z
elseif m == 6
  H = Z .^6 - 15*Z .^4 + 45*Z .^2 - 15
elseif m == 7
  H = Z .^7 - 21*Z .^5 + 105*Z .^3 - 105*Z
elseif m == 8
  H = Z .^8 - 28*Z .^6 + 210*Z .^4 - 420*Z .^2 + 105
elseif m == 9
  H = Z .^9 - 36*Z .^7 + 378*Z .^5 - 1260*Z .^3 + 945*Z
elseif m == 10
  H = Z .^10 - 45*Z .^8 + 630*Z .^6 - 3150*Z .^4 + 4725*Z .^2
      - 945
elseif m == 11
  H = Z .^11 - 55*Z .^9 + 990*Z .^7 - 6930*Z .^5 + 17325*Z .^3
      - 10395*Z
elseif m == 12
  H = Z .^12 - 66*Z .^10 + 1485*Z .^8 - 13860*Z .^6
      + 51975*Z .^4 - 62370*Z .^2 + 10395
end
% ============================================================
```

LIST OF REFERENCES

1. W.B. Davenport and W.L. Root, *An Introduction to the Theory of Random Signals and Noise*, pp. 250-256, McGraw-Hill, New York, 1958.

2. J.I. Marcum, "A statistical theory of target detection by pulsed radar, Mathematical Appendix," *IRE Trans. on Information Theory*, Vol. IT-6, pp. 145-267, 1960.

3. M.I. Skolnik, *Introduction to Radar Systems*, 2nd Edition, pp. 20-60, McGraw-Hill, New York, 1980.

4. D.P. Meyer and H.A. Mayer, *Radar Target Detection, Handbook of Theory and Practice*, pp. 19-34, Academic Press, New York, 1973.

5. D.K. Barton, *Radar System Analysis*, pp. 11-34, pp. 128-131, Prentice-Hall, Englewood Cliffs, New Jersey, 1964.

6. M. Schwarz, *Information Transmission, Modulation, and Noise*, 3rd Edition, pp. 362-363, McGraw-Hill, New York, 1980.

7. R.C. Emerson, "First probability densities for receivers with square law detectors," *Journal of Applied Physics*, Vol. 24, No. 9, pp. 1168-1175, 1953.

8. M.G. Kendall, A. Stuart, and J.K. Ord, *Kendall's Advanced Theory of Statistics*, 5th Edition, pp. 84-89, Oxford University Press, New York, 1987.

9. M. Abramowitz and I.A. Stegun, *Handbook of Mathematical Functions*, pp. 927-935, U.S. Deptartment of Commerce, National Bureau of Standards, Applied Mathematics Series 55, Washington, 1964.

10. A.D. Whalen, *Detection of Signals in Noise*, pp. 246-258, Academic Press, San Diego, 1971.

11. H. Cramer, *Mathematical Methods of Statistics*, pp. 208-230, Princeton University Press, Princeton, 1946.

12. W.H. Beyer, *CRC Standard Mathematical Tables*, 28th Edition, pp. 297, 292-293, CRC Press, Boston, 1990.

13. B. Spain and M.G. Smith, *Functions of Mathematical Physics*, pp. 187-193, Van Nostrand Reinhold Company, London, 1970.

INITIAL DISTRIBUTION LIST

1.	Defense Technical Information Center Cameron Station Alexandria, Virginia 22304-6145	2
2.	Library, Code 52 Naval Postgraduate School Monterey, California 93943-5000	2
3.	Department Chairman, Code EC Department of Electrical and Computer Engineering Naval Postgraduate School Monterey, California 93943-5000	1
4.	Professor Donald v.Z. Wadsworth, Code EC/Wd Department of Electrical and Computer Engineering Naval Postgraduate School Monterey, California 93943-5000	1
5.	Professor Ralph Hippenstiel, Code EC/Hi Department of Electrical and Computer Engineering Naval Postgraduate School Monterey, California 93943-5000	1
6.	Major Chang Long Wee Air Logistic Department, HQ RSAF MINDEF Building, Gombak Drive Off Upper Bukit Timah Rd Singapore 2366	1

Thesis
C37155 Chang
c.1 Effects of video bandwidth on the performance of a square law detector with Gaussian IF and video filters.